

Electronic Supplementary Information

RGH-MOF as a naked eye colorimetric fluorescent sensor for picric acid recognition

Yihe Zhang,^{a,b} Bin Li,^{a*} Heping Ma^{a*} Liming Zhang,^a Wenxiang Zhang^{a,b}

^aState Key Laboratory of Luminescence and Applications, Changchun Institute of Optics Fine Mechanics and Physics, Chinese Academy of Sciences, Changchun 130033, P. R. China

^bUniversity of Chinese Academy of Sciences, Beijing 100039, P. R. China

E-mail: libinteacher@163.com (B. Li)

mahp@ciomp.ac.cn (H. Ma)

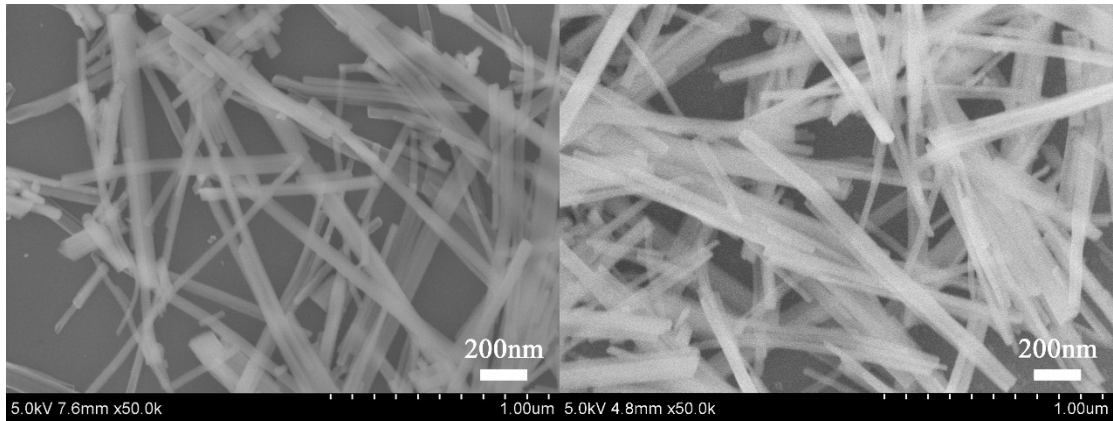


Fig. S1. SEM images of (a) Eu(BTC) and (b) RGH-Eu(BTC).

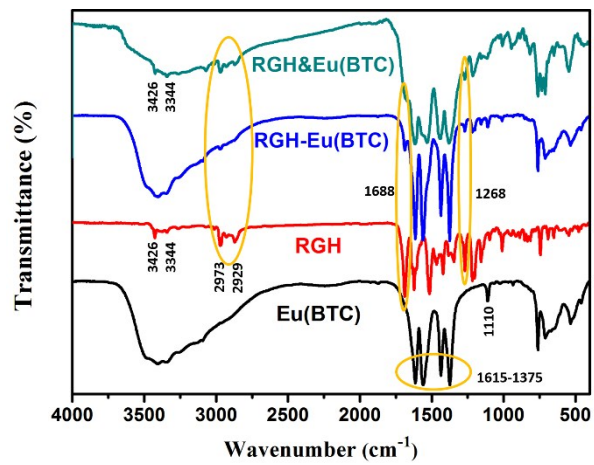


Fig. S2. FTIR spectra of Eu(BTC), RGH, RGH-Eu(BTC) and RGH&Eu(BTC).

Table S1. Elemental analyses of RGH-Eu(BTC)

Sample	C (wt%)	N (wt%)
Eu(BTC)	23.44	0.29
RGH-Eu(BTC)	31.41	1.77

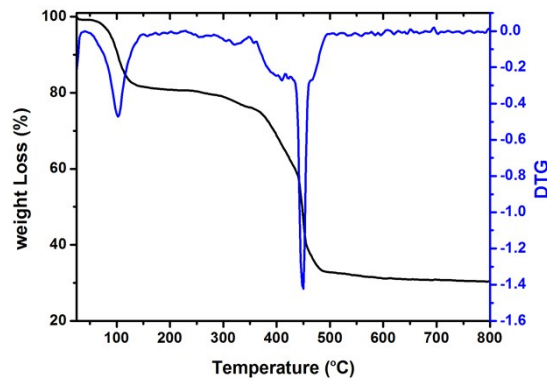


Fig. S3. Thermogravimetric curve of RGH-Eu(BTC).

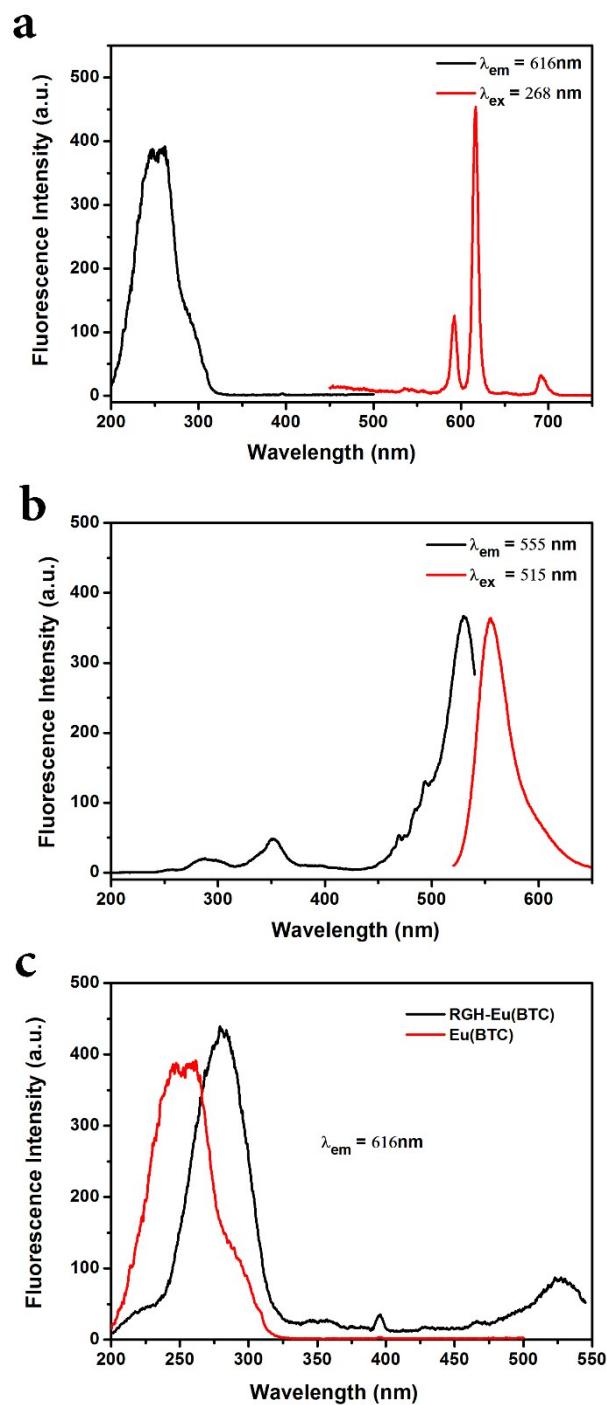


Fig. S4. The fluorescent excitation and emission spectra of (a) Eu(BTC); and (b) RGH+PA. (c) Fluorescent excitation of Eu(BTC) and RGH-Eu (BTC).

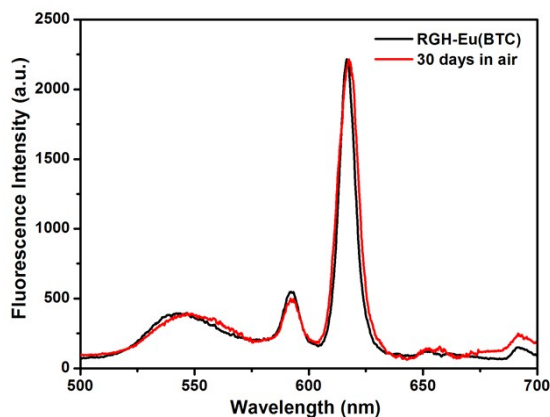


Fig. S5. Fluorescence spectra of the original RGH-Eu(BTC) (black line) and exposed in air for 30 days (red line).

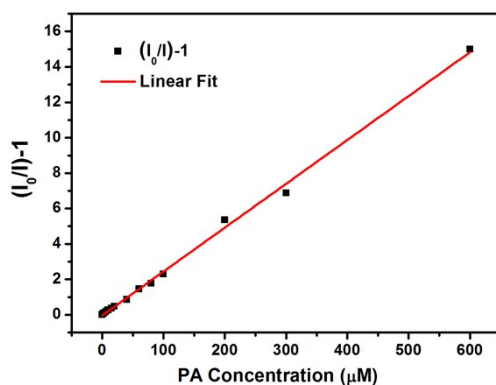


Fig. S6. The linear response of the integrated intensity of Eu(BTC) and PA concentration, excited at 285 nm.

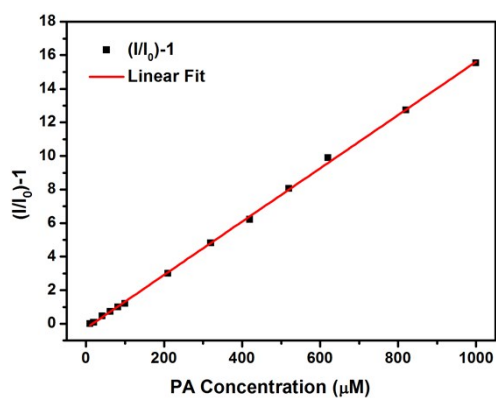


Fig. S7. The linear response of the integrated intensity of RGH and PA concentration, excited at 510 nm.

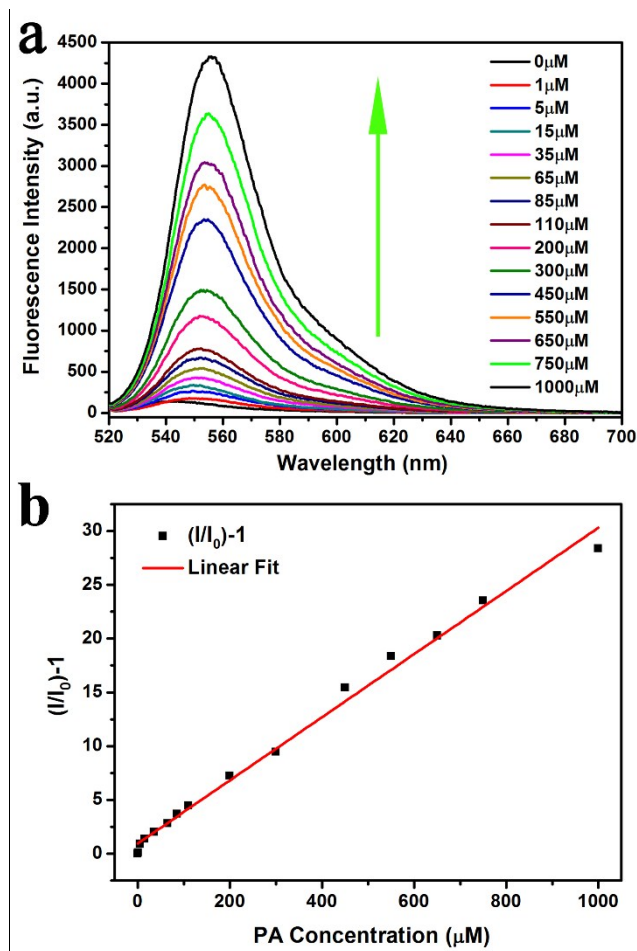


Fig. S8. (a) Fluorescence spectra of RGH-Eu(BTC) with different concentrations of PA when excited at 510 nm. (b) Corresponding linear fitting plot of RGH-Eu(BTC).

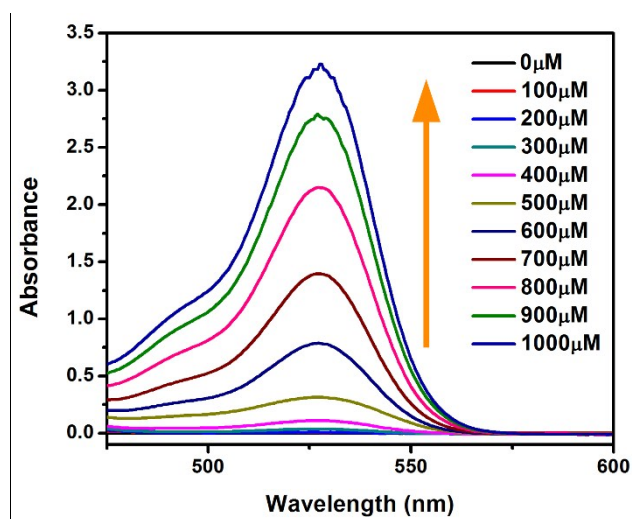


Fig. S9. Absorption spectra of RGH (50 μM) in the presence of various concentration of PA.

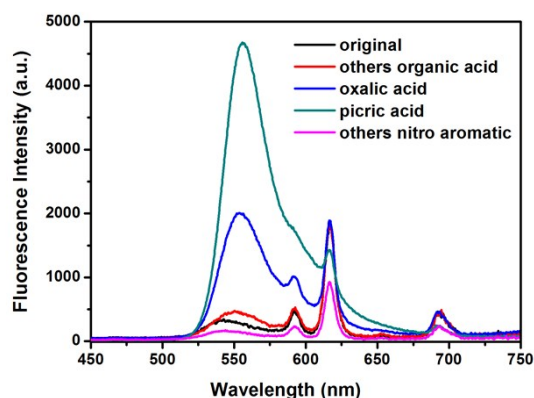


Fig. S10. Emission spectra of RGH-Eu(BTC) (0.05 mg/mL) in the presence of equivalent PA and various analytes in ethanol.

Table S2. Average values and RSD data of I_{555}/I_{616} upon addition of different analytes

	Addition individual		Coexistence with PA	
	Average value of I_{555}/I_{616}	RSD (n=3) (%)	Average value of I_{555}/I_{616}	RSD (n=3) (%)
Blank	0.21391	9.822	0.21391	2.878
Ac	0.25641	6.688	0.25641	2.01
Ox	1.05449	2.669	1.05449	3.436
Ma	0.312	6.7665	0.312	3.038
phenol	0.20253	9.4075	0.20253	2.968
BA	0.24578	10.443	0.24578	4.502
4-NT	0.36831	6.5865	0.36831	5.662
Cl-NB	0.19485	7.975	0.19485	2.63
2,4-DNT	0.19374	12.1015	0.19374	2.182
NB	0.29367	8.7095	0.29367	6.228
3-NP	0.22916	9.4205	0.22916	2.612
TNT	0.23782	8.0015	0.23782	3.796

Table S3. HOMO and LUMO energies for several electron deficient nitro aromatic calculated by density functional theory at B3LYP/6- 31G* level.

Analytes	HOMO (eV)	LUMO (eV)	Band gap (eV)
NT	-7.68	-2.789	4.891
Cl-NB	-7.862	-3.105	4.757
2,4-DNT	-8.0139	-2.9607	5.0532
NB	-7.587	-2.425	5.162
3-NP	-7.223	-2.969	4.254
TNT	-8.3350	-3.5729	4.7621
PA	-8.2915	-3.8750	4.4165

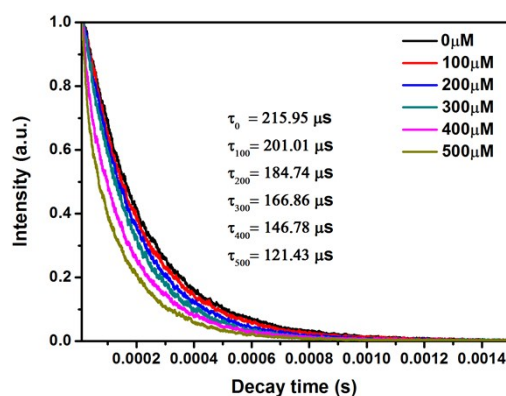


Fig. S11. Fluorescence decay curve of Eu(BTC) upon addition of PA.

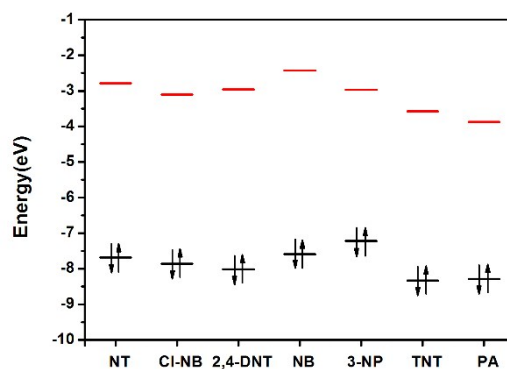


Fig. S12. HOMO and LUMO energies for several electron deficient nitro aromatic.

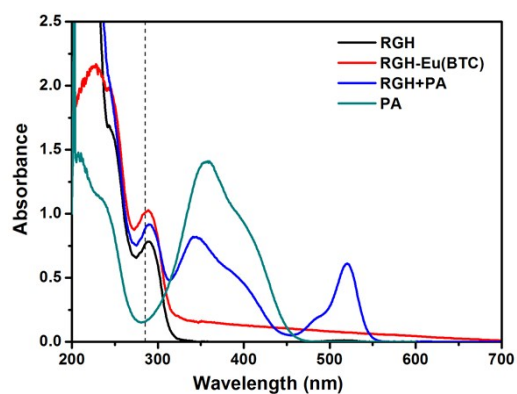


Fig. S13. The absorption spectra of RGH, RGH-Eu(BTC), RGH+PA and PA.

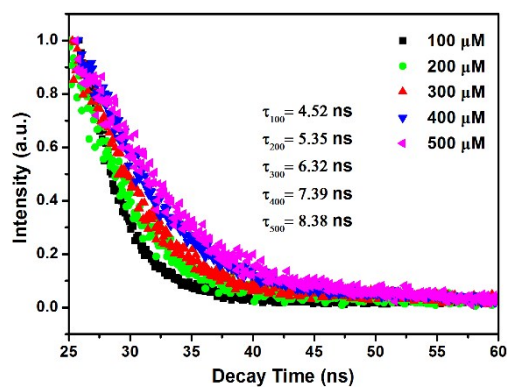


Fig. S14. Fluorescence decay curves of RGH with different PA concentration (100-500 μM), excited at 285 nm.

Table S4. The pKa values of organic acids in this work.

Acids	pKa	Acids	pKa
Picric acid	0.38	Acetic acid	4.76
Oxalic acid	1.25	Malonic acid	2.83
Phenol	9.95	Benzoic acid	4.19